DOI: 10.1002/zaac.200700179

Syntheses, Crystal Structures, and Optical and Magnetic Properties of Some $CsLnCoQ_3$ Compounds (Ln = Tm and Yb, Q = S; Ln = Ho and Yb, Q = Se)

George H. Chan, Leif J. Sherry, Richard P. Van Duyne, and James A. Ibers*

Evanston, IL/USA, Northwestern University, Department of Chemistry

Received January 6th, 2007.

Dedicated to Professor Welf Bronger on the Occasion of his 75th Birthday

Abstract. The four new compounds $CsTmCoS_3$, $CsYbCoS_3$, $CsHoCoSe_3$, and $CsYbCoSe_3$ have been synthesized at 1123 K. These black-colored isostructural compounds crystallize in the $KZrCuS_3$ structure type with four formula units in space group *Cmcm* of the orthorhombic system. The structure of these compounds is composed of $^2_\infty[LnCoQ_3^-]$ layers separated by Cs atoms. Because there are no Q−Q bonds, the formal oxidation states of Cs/Ln/Co/Q are 1+/3+/2+/2−, respectively. $CsHoCoSe_3$ shows paramagnetic behavior with μ_{eff} = 11.9(1) μ_B, whereas $CsYbCoS_3$ displays an antiferromagnetic-like transition at ~2.7 K with μ_{eff} = 5.85(1) μ_B. Both $CsYbCoS_3$ and $CsYbCoSe_3$ exhibit optical band gaps in the near infrared region and broad absorption bands at lower energies.

Keywords: Cobalt; Rare earth; Chalcogenides; Solid-state chemistry; Crystal structures; Optical properties; Magnetic properties

1 Introduction

Many $AM'MQ_3$ and $AkM'MQ_3$ compounds (A = alkali metal, Ak = alkaline-earth metal, M′= lanthanide or actinide, M = transition metal, Q = S, Se, or Te) (Table 1) possessing the $KZrCuS_3$ structure type [1] have been synthesized by means of the reactive-flux method [2]. Many of these isostructural compounds have been discovered by means of simple chemical substitution of M′, M, or Q. These compounds show varied and interesting physical properties. Some examples include: $KUCuSe_3$ [3], a narrow gap p-type semiconductor with electrical conductivity as high as 0.1 S/cm at 300 K; $CsCeCuS_3$ [3], a paramagnetic p-type semiconductor with an electrical conductivity of 1 S/cm at 298 K and the unusual formal valence representation $Cs^{1+}Ce^{3+}Cu^{1+}(S^{2-})_2(S^{1-})$; and $EuM'CuS_3$ [4] (M′ = Tm−Lu) that display ferromagnetic or ferrimagnetic transitions at low temperatures.

Both from experiment and first-principles electronic structure calculations, it is found that the band gaps of the $ALnMQ_3$ materials (A = Rb, Cs; Ln = rare-earth metal; M = Mn, Zn, Cd, Hg) can be tuned through simple chemical substitution of Ln, M, or Q [5−7]. For some of these compounds, there is also a slight dependence of band gap on crystal orientation [5, 8]. Most of these compounds show Curie-Weiss behavior [7], except for the compounds Ln = Yb/M = Mn, Zn that show magnetic transitions at temperatures below ~10 K. Thus these $ALnMQ_3$ compounds are a new class of magnetic semiconductors with tunable band gaps that show potential applications in magnetic storage devices [9, 10] and photonic devices such as optical waveguides [11], optical filters [12], spontaneous emitters [13], and photon traps [14]. However, no $ALnMQ_3$ compounds containing a magnetic transition metal such as Fe, Ni, or Co have been successfully prepared to date. Yet incorporation of a magnetic transition metal may lead to different magnetic properties.

Here we report the syntheses, crystal structure, optical, and magnetic properties of four new $CsLnCoQ_3$ compounds, namely $CsTmCoS_3$, $CsYbCoS_3$, $CsHoCoSe_3$, and $CsYbCoSe_3$.

Table 1 Tabulation of M′ elements for known $AM'MQ_3$ compounds of the $KZrCuS_3$ structure type

Compound	Q = S	Q = Se	Q = Te	Reference
$KM'CuQ_3$	Zr, Th	Zr, U, Th	Zr	[1, 3, 36, 37]
$CsM'CuQ_3$	Ce	Zr, U, Th	U	[3, 30, 35, 37]
$BaM'CuQ_3$	Er	Gd	Y, Dy	[30−33]
$BaM'AgQ_3$		Y	Y	[31, 32]
$BaM'AuQ_3$		Gd		[32]
$CsM'MnQ_3$		Sm−Yb, Y		[7]
$CsM'ZnQ_3$	Yb	Sm−Yb, Y	La−Yb, Y	[6−8]
$CsM'CdQ_3$		Ce−Dy, Y		[5]
$CsM'HgQ_3$		La−Gd, Y		[5]
$RbM'ZnQ_3$		Yb	Yb	[7]
$SrM'CuQ_3$		Lu		[34]

* Prof. James A. Ibers
Department of Chemistry
Northwestern University
2145 Sheridan Rd.
Evanston, IL 60208-3113, USA
Tel: +1 847 491 5449
Fax: +1 847 491 2976
E-Mail: ibers@chem.northwestern.edu

2 Experimental Part

Syntheses. The following reagents were used as received: Cs (Aldrich, 99.5 %), Ho (Alfa Aesar, 99.9 %), Tm (Strem, 99.9 %), Yb (Strem, 99.9 %), CoS (Alfa Aesar, 99.5 %), CoSe (Alfa Aesar, 99+ %), S (Alfa Aesar, 99.99 %), Se (Cerac, 99.99 %), CsCl (Strem, 99.999 %), and CsI (Aldrich 99.99 %). Cs_2Q_3 (Q = S, Se), the reactive fluxes [2] employed in the syntheses, were prepared by the stoichiometric reactions of the elements in liquid NH_3. Reaction mixtures were loaded into carbon-coated fused-silica tubes in an Ar filled glovebox. These tubes were sealed under a 0.013 Pa atmosphere and then placed in a computer-controlled furnace. Upon completion of the heating and cooling cycle, each reaction mixture was washed with de-ionized water and dried with acetone. The $CsLnCoQ_3$ compounds are stable in air.

Black needles of $CsLnCoS_3$ (Ln = Tm, Yb) were obtained from the reaction of 0.3 mmol of Cs_2S_3, 0.5 mmol of CoS, 0.5 mmol of Ln, and 0.5 mmol of S; 150 mg of CsI were added to promote crystallization. The samples were heated to 773 K in 7 h, kept at 773 K for 24 h, heated to 1123 K in 24 h, kept at 1123 K for 96 h, cooled at 4 K/h to 573 K, and then the furnace was turned off. Generally, the yields of these compounds were 50−70 % based on Ln.

Black needles $CsLnCoSe_3$ (Ln = Ho, Yb) were obtained from the reaction of 0.3 mmol of Cs_2Se_3, 0.5 mmol of CoSe, 0.5 mmol of Ln, and 0.5 mmol of Se; 150 mg CsCl were added to promote crystal growth. The samples were heated to 1123 K in 48 h, kept at 1123 K for 50 h, cooled at 4 K/h to 573 K, and then the furnace was turned off. The yields of these compounds were 50−60 % based on Ln.

Energy-Dispersive X-ray (EDX) analyses were carried out with the use of an Hitachi S-3500 SEM. Data were collected with an accelerating voltage of 20 keV, a working distance of 15 mm, and a collection time of 60 s. Selected single crystals of $CsTmCoS_3$, $CsYbCoS_3$, $CsHoCoSe_3$, and $CsYbCoSe_3$ showed the presence of Cs, Ln, Co, and Q at an approximate ratio of 1:1:1:3. No evidence for the presence of Cl or I was found.

Single-crystal X-ray diffraction data for $CsTmCoS_3$, $CsYbCoS_3$, $CsHoCoSe_3$, and $CsYbCoSe_3$ were collected on a Bruker Smart 1000 CCD diffractometer [15] at 153 K with the use of monochromatized Mo Kα radiation (λ = 0.71073 Å). The crystal-to-detector distance was 5.023 cm. Crystal decay was monitored by recollecting 50 initial frames at the end of the data collection. The diffracted intensities were generated by a scan of 0.3° in ω in groups of 606 frames for each of the φ settings 0°, 90°, 180°, and 270°. The exposure times varied from 15 to 20 s/frame. Intensity data were collected with the program SMART [15]. For each compound, cell refinement and data reduction were carried out with the program SAINT [15] and a numerical face-indexed absorption correction was made with the use of the program XPREP [16]. Finally, the program SADABS [16] was employed to make incident beam and decay corrections.

The crystal structures were solved in space group *Cmcm* of the orthorhombic system with the direct-methods program SHELXS [16] and refined anisotropically with the full-matrix least-squares program SHELXL [16]. The program STRUCTURE TIDY [17] was used to standardize the positional parameters. Additional crystallographic details are given in Table 2 and in Supporting Information. Table 3 presents selected metrical data for $CsTmCoS_3$, $CsYbCoS_3$, $CsHoCoSe_3$, and $CsYbCoSe_3$.

DC magnetic susceptibility measurements were carried out with the use of a Quantum Design MPMS5 SQUID magnetometer. The composition of a given sample was verified by EDX measurements. Single crystals of $CsHoCoSe_3$, (23.7 mg) and $CsYbCoS_3$ (5.4 mg) were ground and loaded into gelatin capsules. In the temperature range 5−300 K for $CsHoCoSe_3$ and 1.8−380 K for $CsYbCoS_3$, both zero-field cooled (ZFC) and field cooled (FC) measurements were carried out with an applied field of 500 G (0.05 T). The susceptibility data were corrected for core diamagnetism [18]. The inverse molar susceptibility χ_m^{-1} in the temperature range 100−300 K for $CsHoCoSe_3$ (ZFC) and 100−380 K for $CsYbCoS_3$ (ZFC) was fit by a least-squares method to the Curie-Weiss equation $\chi_m^{-1} = (T-\theta_p)/C$, where C is the Curie constant and θ_p is the Weiss constant. The effective magnetic moment μ_{eff} was calculated from the equation $\mu_{eff} = (7.997C)^{1/2}\,\mu_B$ [19].

Single-crystal absorption measurements over the range 900 nm (1.38 eV) to 1700 nm (0.73 eV) at 293 K were performed on a single crystal of $CsYbCoS_3$ with the use of a Nikon TE300 inverted microscope coupled by a fiber optic to a near-infrared spectrometer (128L-1.7T1, T.E. Cooled InGaAs Array). The selected single crystal of $CsYbCoS_3$ was face-indexed and its crystal dimensions were measured by means of the video attachment on a Bruker Smart-1000 CCD diffractometer. Crystal dimensions were [100], [010], [001]: 120, 24, 20 μm, respectively. The single crystal was positioned at the focal point above a 20 x objective with the use of a goniometer mounted on a translation stage (Line Tool Company). Fine alignment of the microscope assembly was achieved by maximizing the transmission of the lamp profile. Unpolarized light originating from a tungsten-halogen lamp impinged on the crystal and the

Table 2 X-ray crystallographic data for $CsLnCoQ_3$[a]

Formula	$CsTmCoS_3$	$CsYbCoS_3$	$CsHoCoSe_3$	$CsYbCoSe_3$
fw	456.95	461.06	593.65	601.76
a (Å)	3.9452(5)	3.9317(4)	4.1076(3)	4.0669(3)
b (Å)	15.231(2)	15.2281(15)	15.7664(11)	15.7594(13)
c (Å)	10.4179(15)	10.3984(10)	10.8464(8)	10.7666(9)
V (Å^3)	625.99(15)	622.58(11)	702.44(9)	690.05(10)
ρ_{calc} (g cm^{-3})	4.849	4.919	5.613	5.792
μ (cm^{-1})	233.14	242.13	340.64	367.62
$R(F)$[b]	0.0381	0.0293	0.0177	0.0293
$R_w(F_o^2)$[c]	0.0849	0.0649	0.0415	0.0670
q	0.04	0.03	0.02	0.03

[a] For all structures Z = 4, T = 153(2) K, space group = *Cmcm* and λ = 0.71073 Å.
[b] $R(F) = \Sigma\|\|F_o|-|F_c\|\,/\,|F_o|$ for $F_o^2 > 2\sigma(F_o^2)$.
[c] $R_w(F_o^2) = \{\Sigma\,[w(F_o^2-F_c^2)^2]\,/\,\Sigma wF_o^4\}^{1/2}$ for all data. $w^{-1} = \sigma^2(F_o^2) + (qP)^2$, where $P = \max(F_o^2,0)$.

Table 3 Selected distances /Å and angles /deg. for $CsLnCoQ_3$

Atoms	$CsTmCoS_3$	$CsYbCoS_3$	$CsHoCoSe_3$	$CsYbCoSe_3$
Cs−Q1 x 4	3.584(2)	3.589(2)	3.6684(4)	3.6677(8)
Cs−Q1 x 2	3.745(2)	3.740(2)	3.8793(5)	3.8477(8)
Cs−Q2 x 2	3.491(3)	3.486(2)	3.5936(6)	3.586(1)
Ln−Q1 x 4	2.703(2)	2.689(1)	2.8459(3)	2.8136(5)
Ln−Q2 x 2	2.7107(9)	2.7065(7)	2.8384(2)	2.8193(4)
Co−Q1 x 2	2.296(3)	2.298(2)	2.4227(6)	2.422(1)
Co−Q2 x 2	2.375(2)	2.365(2)	2.4958(6)	2.478(1)
Q1−Co−Q1	118.9(1)	119.1(1)	116.27(4)	117.11(7)
Q1−Co−Q2	106.44(4)	106.37(3)	107.454(7)	107.35(1)
Q2−Co−Q2	112.3(1)	112.4(1)	110.75(4)	110.27(7)
Q1−Ln−Q1	93.75(7)	93.98(5)	92.39(1)	92.56(2)
Q1−Ln−Q2	92.55(7)	92.42(5)	91.52(1)	91.00(2)

transmitted light was then spatially filtered before being focused into the 400 μm core diameter fiber coupled to the spectrometer. The absorbance spectra of light perpendicular to both the (010) and (001) crystal faces of $CsYbCoS_3$ were collected. The optical band gaps were calculated by means of a linear regression technique described previously [5].

Diffuse reflectance spectra over the range 200 nm (6.21 eV) to 2600 nm (0.48 eV) at 298 K of $CsYbCoSe_3$ were obtained with a Varian Cary 5000 UV-vis/NIR double-beam spectrometer equipped with a diffuse reflectance accessory. The sample was prepared from selected single crystals of $CsYbCoSe_3$ that were ground into a fine powder and inserted into a customized sample holder. The absorption (α/S) data were calculated from the reflectance data with the use of the Kubelka-Munk function $\alpha/S = (1-R)^2/2R$, where R is the reflectance at a given energy, α is the absorption coefficient, and S is the scattering coefficient [20].

3 Results and Discussion

3.1 Syntheses

The compounds $CsTmCoS_3$, $CsYbCoS_3$, $CsHoCoSe_3$, and $CsYbCoSe_3$ were obtained in 50−70 % yields from the reactions of Ln, CoQ, Q, and Cs_2Q_3 at 1123 K. The trends of Ln radius vs. M radius discovered in previous syntheses of $CsLnMSe_3$ [5, 7, 8] persist here. Thus, the $CsLnCoS_3$ materials could only be obtained for the smaller rare-earth elements Tm and Yb, whereas the $CsLnCoSe_3$ materials could be obtained over a greater range of Ln radii, namely for Ln = Sm, Gd, Tb, Er, Ho, Tm, Yb, and Y, as confirmed by EDX and powder diffraction measurements. However, only for Ho and Yb were crystals obtained that were suitable for single-crystal X-ray diffraction studies. SEM microscopy indicated that the crystals of the other compounds were made up of bundles of thin needles.

3.1 Crystal Structure

The isostructural compounds $CsTmCoS_3$, $CsYbCoS_3$, $CsHoCoSe_3$, and $CsYbCoSe_3$ possess the $KZrCuS_3$ structure type [1], crystallizing with four formula units in space group *Cmcm* of the orthorhombic system. The unit cell of $CsLnCoQ_3$ is illustrated in Figure 1. Each Cs atom (site symmetry *mm*) is coordinated to eight Q atoms to form a bicapped trigonal prism; each Ln atom (site symmetry 2/*m*) is coordinated to six Q atoms to form a distorted octahedron; and each Co atom (site symmetry *mm*) is coordinated to four Q atoms to form a distorted tetrahedron. Each CoQ_4 tetrahedron shares edges with four LnQ_6 octahedra along [001] to form a two-dimensional $^2_\infty[LnCoQ_3^-]$ layer. These layers, which stack perpendicular to [010] (Fig. 2), are separated by Cs atoms. These in turn form a layer composed of face- and edge-sharing CsQ_8 bicapped trigonal prisms. Each CsQ_8 prism has two face-sharing

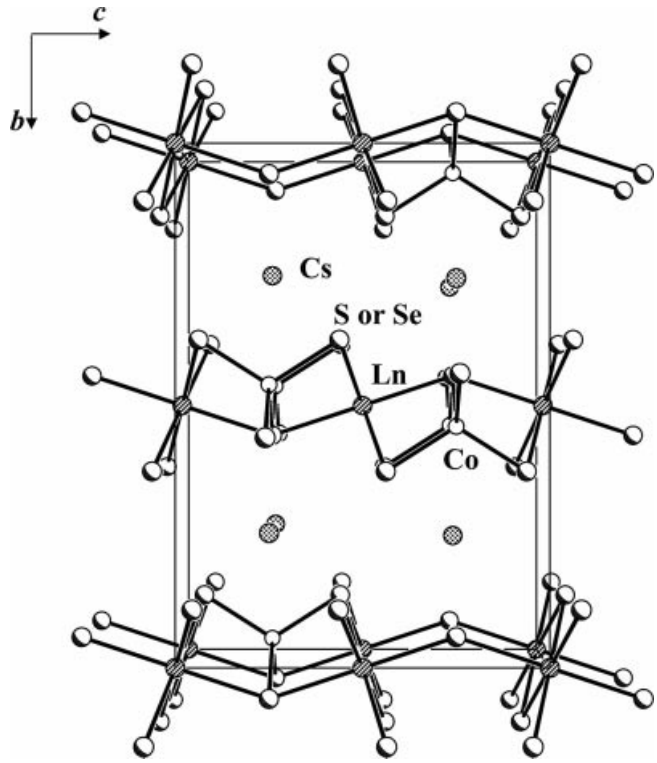

Figure 1 Unit cell of $CsLnCoQ_3$.

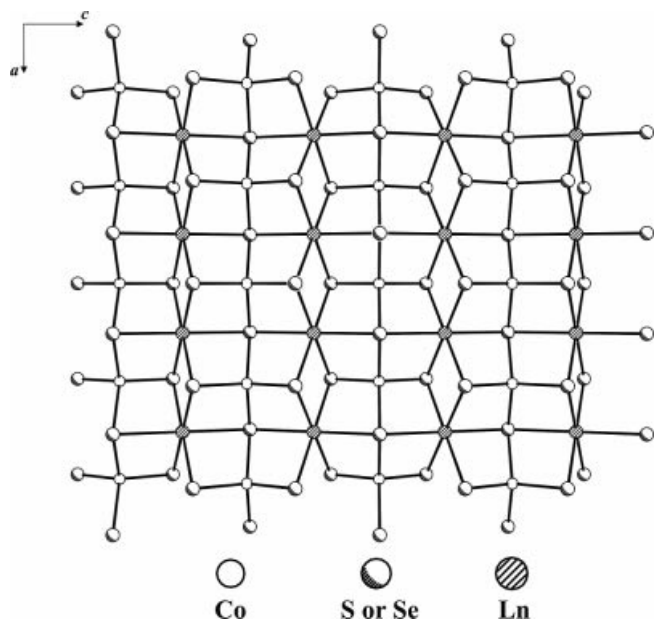

Figure 2 $^2_\infty[LnCoQ_3^-]$ layer viewed down [010].

neighbors along [100] and four edge-sharing ones along [001] to form a $^2_\infty[CsQ_3]$ layer in the *ac* plane. Each LnQ_6 octahedron edge shares with two other octahedra along [100] to form a one dimensional $^1_\infty[LnQ_4]$ chain. The MQ_4 tetrahedra share vertices with two neighboring tetrahedra along [100] to form a one-dimensional $^1_\infty[MQ_3]$ chain. Note,

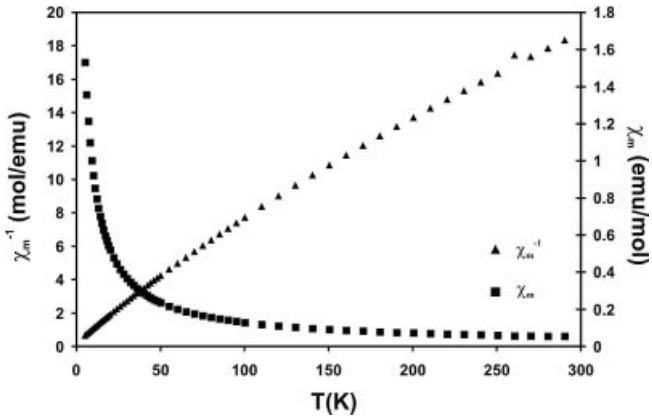

Figure 3 Molar magnetic susceptibility χ_m and inverse molar magnetic susceptibility $\chi_m{}^{-1}$ vs. T of $CsHoCoSe_3$ for ZFC data. FC data (not shown) are very similar.

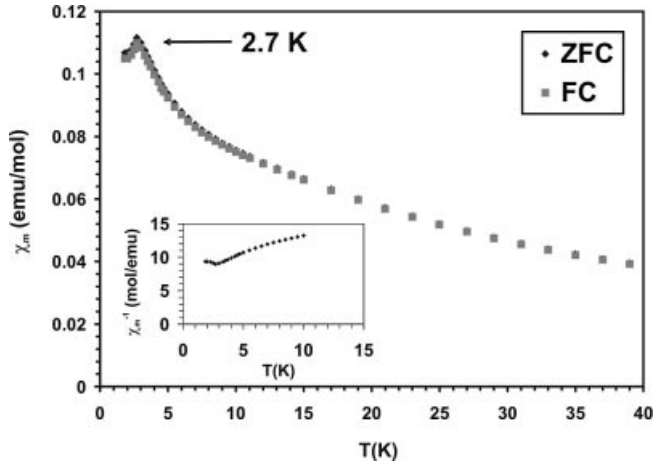

Figure 4 Molar magnetic susceptibility χ_m vs. T for $CsYbCoS_3$ for ZFC and FC data. Inset is a plot of molar magnetic susceptibility $\chi_m{}^{-1}$ vs. T (ZFC data).

each Q1 atom is bonded to two Ln atoms and three Cs atoms, whereas each Q2 atom is bonded to two M atoms, one Ln atom, and two Cs atoms. Because there are no Q−Q bonds in the structure, the formal oxidation states of Cs/Ln/Co/Q are 1+/3+/2+/2−, respectively. These materials are valence precise and are expected to be semiconductors.

Selected metrical data for $CsTmCoS_3$, $CsYbCoS_3$, $CsHoCoSe_3$, and $CsYbCoSe_3$ are displayed in Table 3. These bond lengths are consistent, for example, with those of 2.735(6) Å for Tm−S in $CsTmS_2$ [21]; 2.677(2) −2.694(2) Å for Yb−S in $CaYbInS_4$ [22]; 2.839(1) Å for Ho−Se in $CdHo_2Se_4$ [23]; 2.752(3) −2.934(2) Å for Yb−Se in $Rb_3Yb_7Se_{12}$ [24]; 3.532(3) −3.861(2) Å for Cs−S in $Cs_2Au_2Cd_2S_4$ [25]; 3.4281(8) −3.9527(3) Å for Cs−Se in $CsSm_2CuSe_4$ [26]; 2.365(2) Å for Co−S in Cs_2CoS_2 [27]; and 2.473(2) Å for Co−Se in Cs_2CoSe_2 [27]. Consistent with the trends seen earlier, distortions from ideal symmetry of the LnQ_6 octahedra and MQ_4 tetrahedra are greater for Q = S than for Q = Se. Such distortions may affect the degree of magnetic coupling between Co^{2+} and Ln^{3+}.

3.3 Magnetic Properties

The molar magnetic susceptibility χ_m and its inverse $\chi_m{}^{-1}$ of $CsHoCoSe_3$ (ZFC) as a function of temperature are illustrated in Figure 3. FC and ZFC susceptibility data for $CsHoCoSe_3$ are very similar and do not show evidence for magnetic ordering between 5 to 300 K. The compound is paramagnetic, obeying Curie-Weiss behavior $\chi_m{}^{-1} = (T-\theta_p)/C$, in the temperature region 100 −300 K with values of C = 17.98(1) emu K mol^{-1}, θ_p = −43.84(3) K, and μ_{eff} = 11.9(1) μ_B. Below 100 K there is a slight deviation from Curie-Weiss behavior as a result of crystal-field effects [28].

The compounds $CsHoZnSe_3$ [8] and $CsHoMnSe_3$ [7] are Curie-Weiss paramagnets with μ_{eff} values of 10.55(1) and 12.23(7) μ_B, respectively. The theoretical values are 10.6 and 12.1 μ_B, respectively [29]. The results for $CsHoMnSe_3$ are consistent with the presence of high-spin Mn^{2+} where the crystal field is assumed to be in an ideal tetrahedral state. In contrast, comparison of the experimental and calculated μ_{eff} values of 11.9(1) μ_B vs. 12.50 μ_B (L-S coupling) or 11.28 μ_B (spin only) for the present compound $CsHoCoSe_3$ indicates that the orbital magnetic moment of Co^{2+} is quenched. What the spin state of Co^{2+} is in this compound is unclear; both high-spin and low-spin states contribute to a total of three unpaired spins.

Figure 4 shows $\chi_m{}^{-1}$ vs. T (both FC and ZFC) for $CsYbCoS_3$. As distinct from results for the previously studied $AYbMQ_3$ (M = Mn, Zn) compounds [7, 8], the FC and ZFC data are very similar and there is a sharp magnetic transition at ~ 2.7 K. Curie-Weiss behavior is observed in the temperature region of 100−380 K with values of C = 4.29(2) emu K mol^{-1}, θ_p = −102.54(5) K, and μ_{eff} = 5.85(1) μ_B. The calculated values of μ_{eff} are 8.03 μ_B (L-S coupling) and 5.96 μ_B (spin-only) [29]. Hence the orbital moment of Co^{2+} is again quenched. The large negative Weiss constant θ_p of −102.54(5) K indicates considerable antiferromagnetic coupling, presumably between Co^{2+} and Yb^{3+}. Note this θ_p is larger than that of −89.9(4) K in $CsYbMnSe_3$ [7]. Thus the coupling between Yb^{3+} and Co^{2+} in $CsYbCoS_3$ is probably greater than that between Yb^{3+} and Mn^{2+} in $CsYbMnSe_3$ and is consistent with the shortest Yb−Co distance of 3.307(3) Å being less than the shortest Yb−Mn distance of 3.4874(5) Å. Note a broad magnetic transition was observed in $CsYbMnSe_3$.

3.4 Optical Properties

From the absorption spectra of $CsYbCoS_3$ (Fig. 5), direct optical transitions of 1.15 eV for the (010) crystal face and 1.18 eV for the (001) crystal face were derived. This variation in optical transition with crystal orientation is minimal, whereas in $CsYZnSe_3$ and $CsSmZnSe_3$ variations with crystal orientation of 0.1 to 0.2 eV were observed (Table 4).

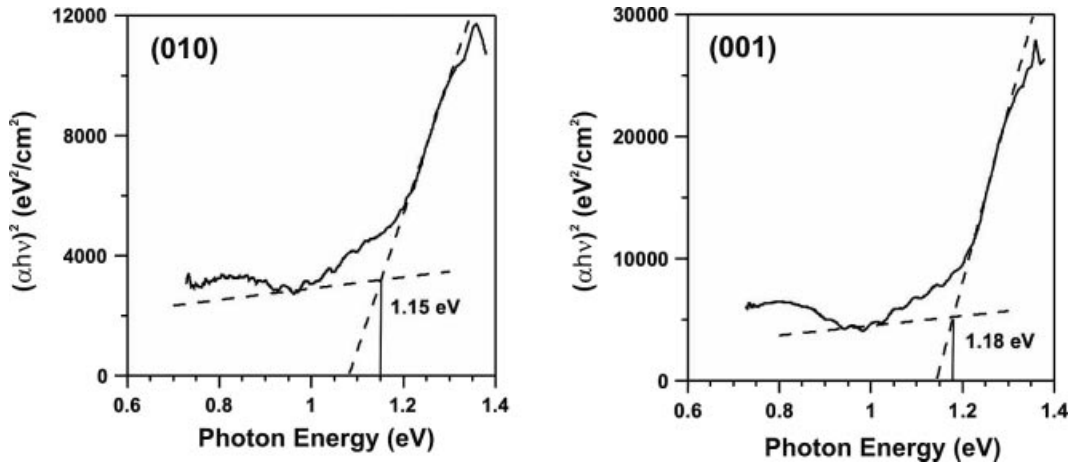

Figure 5 Optical band gaps of $CsYbCoS_3$ for the (010) crystal face and the (001) crystal face.

Table 4 Single-crystal optical band gaps /eV of $ALnMQ_3$ materials

Compound	Color	(010) face	(001) face	Reference
$CsYbCoS_3$	black	1.15	1.18	This work
$CsYbMnSe_3$	red-brown	1.6	1.59	[7]
$CsCeHgSe_3$	red	1.94		[5]
$RbYbZnSe_3$	red	2.07		[7]
$CsYbZnSe_3$	red	2.1	1.97	[5]
$CsTbZnTe_3$	red	2.12	2.12	[6]
$CsGdZnTe_3$	red	2.13		[6]
$CsSmHgSe_3$	yellow	2.36	2.37	[5]
$CsCeCdSe_3$	yellow	2.4	2.4	[5]
$CsYZnSe_3$	yellow	2.41	2.29	[8]
$CsSmCdSe_3$	yellow	2.47	2.45	[5]
$CsYCdSe_3$	yellow	2.48	2.54	[5]
$CsLaHgSe_3$	amber	2.51	2.46	[5]
$CsYHgSe_3$	yellow	2.58	2.54	[5]
$CsYbZnS_3$	yellow	2.61		[7]
$CsSmZnSe_3$	yellow	2.63	2.43	[8]
$CsErZnSe_3$	yellow	2.63	2.56	[8]

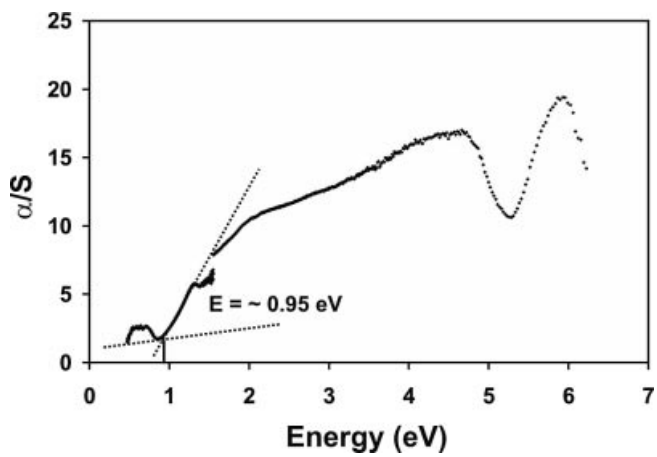

Figure 6 Diffuse reflectance spectrum of $CsYbCoSe_3$.

The colors of the $ALnMQ_3$ materials follow the trends noted earlier and are consistent with the first-principles calculations on $CsYZnSe_3$ [5] and $CsGdZnTe_3$ [6] that showed that the $ALnMQ_3$ materials were direct-band gap semiconductors whose band gaps were governed by the composition of the two-dimensional $^2_\infty[LnMQ_3^-]$ anionic framework. The colors of $CsYbCoQ_3$ (Q = S, Se) are black. From the sequence of energy levels of p orbitals, 3p (S) < 4p (Se) < 5p (Te), the optical band gap of $CsYbCoSe_3$ should be less than that of $CsYbCoS_3$, as observed. The band gap deduced from the diffuse reflectance spectra (Fig. 6) of $CsYbCoSe_3$ is ~ 0.95 eV, which is ~ 0.2 eV less than that in $CsYbCoS_3$. Both compounds exhibit a broad absorption band below their respective optical band gap that may possibly originate from *d-d* transitions of Co. These isostructural materials are valence precise and are semiconductors, as indicated from their optical spectra. Should $CsYbCoTe_3$ be synthesized,it should exhibit a very narrow band gap or perhaps even be metallic.

Supporting material. The crystallographic files in cif format for $CsTmCoS_3$, $CsYbCoS_3$, $CsHoCoSe_3$, and $CsYbCoSe_3$ have been deposited with FIZ Karlsruhe as CSD numbers 417508, 417509, 417507, and 417510, respectively. These data may be obtained free of charge by contacting FIZ Karlsruhe at +49 7247 808 666 (fax) or crysdata@fiz-karlsruhe.de (email)

Acknowledgments. We acknowledge Dr. Hui Yi Zeng, Dr. Jiyong Yao, and Dr. Hiroshi Mizoguchi for their helpful discussions. We thank Mr. Jiha Sung and Prof. Kenneth G. Spears for the use of their NIR spectrometer and Ms. Jill Millstone and Prof. Chad A. Mirkin for the use of their UV-Visible-NIR spectrometer. This research was supported in part by the **National Science Foundation Grant** DMR00-96676 and the **Department of Energy BES Grant** ER-15522. GHC was supported by a Northwestern University MRSEC Fellowship. Use was made of the Central Facilities supported by the **MRSEC program of the National Science Foundation** (DMR00-76097) at the **Materials Research Center of Northwestern University**.

References

[1] M. F. Mansuetto, P. M. Keane, J. A. Ibers, *J. Solid State Chem.* **1992**, *101*, 257−264.
[2] S. A. Sunshine, D. Kang, J. A. Ibers, *J. Am. Chem. Soc.* **1987**, *109*, 6202−6204.
[3] A. C. Sutorik, J. Albritton-Thomas, T. Hogan, C. R. Kannewurf, M. G. Kanatzidis, *Chem. Mater.* **1996**, *8*, 751−761.
[4] M. Wakeshima, F. Furuuchi, Y. Hinatsu, *J. Phys.: Condens. Matter* **2004**, *16*, 5503−5518.
[5] K. Mitchell, F. Q. Huang, A. D. McFarland, C. L. Haynes, R. C. Somers, R. P. Van Duyne, J. A. Ibers, *Inorg. Chem.* **2003**, *42*, 4109−4116.
[6] J. Yao, B. Deng, L. J. Sherry, A. D. McFarland, D. E. Ellis, R. P. Van Duyne, J. A. Ibers, *Inorg. Chem.* **2004**, *43*, 7735−7740.
[7] K. Mitchell, F. Q. Huang, E. N. Caspi, A. D. McFarland, C. L. Haynes, R. C. Somers, J. D. Jorgensen, R. P. Van Duyne, J. A. Ibers, *Inorg. Chem.* **2004**, *43*, 1082−1089.
[8] K. Mitchell, C. L. Haynes, A. D. McFarland, R. P. Van Duyne, J. A. Ibers, *Inorg. Chem.* **2002**, *41*, 1199−1204.
[9] E. P. Wohlfarth. In *Ferromagnetic Materials*; E. P. Wohlfarth, Ed.; North-Holland: New York, 1980; Vol. 1, pp. 1−70.
[10] K. H. J. Buschow. In *Ferromagnetic Materials*; E. P. Wohlfarth, Ed.; North-Holland: New York, 1980; Vol. 1, pp. 297−414.
[11] J. D. Joannopoulos, P. R. Villeneuve, S. Fan, *Nature (London)* **1997**, *386*, 143−149.
[12] Y. Dirix, C. Bastiaansen, W. Caseri, P. Smith, *Adv. Mater.* **1999**, *11*, 223−227.
[13] E. Yablonovitch, *J. Opt. Soc. Am. B* **1993**, *10*, 283−295.
[14] S. Noda, A. Chutinan, M. Imada, *Nature (London)* **2000**, *407*, 608−610.
[15] Bruker. SMART Version 5.054 Data Collection and SAINT-Plus Version 6.45a Data Processing Software for the SMART System; Bruker Analytical X-Ray Instruments, Inc., Madison, WI, USA, 2003.
[16] G. M. Sheldrick. SHELXTL Version 6.14; Bruker Analytical X-Ray Instruments, Inc., Madison, WI, USA, 2003.
[17] L. M. Gelato, E. Parthé, *J. Appl. Crystallogr.* **1987**, *20*, 139−143.
[18] L. N. Mulay, E. A. Boudreaux, Theory and Applications of Molecular Diamagnetism, Wiley-Interscience, New York 1976.
[19] C. J. O'Connor, *Prog. Inorg. Chem.* **1982**, *29*, 203−283.
[20] S. P. Tandon, J. P. Gupta, *Phys. Status Solidi A* **1970**, *37*, 43−45.
[21] W. Bronger, C. Herudek, J. Huster, D. Schmitz, *Z. Anorg. Allg. Chem.* **1993**, *619*, 243−252.
[22] J. D. Carpenter, S.-J. Hwu, *Chem. Mater.* **1992**, *4*, 1368−1372.
[23] K.-J. Range, C. Eglmeier, *J. Alloys Compd.* **1991**, *176*, L13−L16.
[24] S.-J. Kim, S.-J. Park, H. Yun, J. Do, *Inorg. Chem.* **1996**, *35*, 5283−5289.
[25] E. A. Axtell III, M. G. Kanatzidis, *Chem. Eur. J.* **1998**, *4*, 2435−2441.
[26] F. Q. Huang, J. A. Ibers, *J. Solid State Chem.* **2001**, *158*, 299−306.
[27] W. Bronger, C. Bomba, *J. Less-Common Met.* **1990**, *158*, 169−176.
[28] C. Cascales, R. Sáez-Puche, P. Porcher, *J. Solid State Chem.* **1995**, *114*, 52−56.
[29] C. Kittel, Introduction to Solid State Physics, Wiley, New York 1996.
[30] F. Q. Huang, K. Mitchell, J. A. Ibers, *Inorg. Chem.* **2001**, *45*, 5123−5126.
[31] P. Wu, A. E. Christuk, J. A. Ibers, *J. Solid State Chem.* **1994**, *110*, 337−344.
[32] Y. Yang, J. A. Ibers, *J. Solid State Chem.* **1999**, *147*, 366−371.
[33] F. Q. Huang, W. Choe, S. Lee, J. S. Chu, *Chem. Mater.* **1998**, *10*, 1320−1326.
[34] S. Strobel, T. Schleid, *J. Alloys Compd.* **2006**, *418*, 80−85.
[35] J. A. Cody, J. A. Ibers, *Inorg. Chem.* **1995**, *34*, 3165−3172.
[36] H. D. Selby, B. C. Chan, R. F. Hess, K. D. Abney, P. K. Dorhout, *Inorg. Chem.* **2005**, *44*, 6463−6469.
[37] A. A. Narducci, J. A. Ibers, *Inorg. Chem.* **2000**, *39*, 688−691.

